Application of the Leak Before Break(LBB) Concept to a Heat Exchanger in a Nuclear Power Plant

Choon-Yeol Lee, Jae-Do Kwon*, Yong-Son Lee, Il-Chan Sul
School of Mechanical Engineering, Yeungnam University

The leak before break(LBB) concept is difficult to apply to a structure with a thin tube that is immersed in a water environment. A heat exchanger in a nuclear power plant is such a structure. The present paper addresses an application of the LBB concept to a heat exchanger in a nuclear power plant. The minimum leaked coolant amount(approximately 37.9 *liters*) containing the radioactive material which can activate the radiation detector device installed in near the heat exchanger is assumed. A postulated initial flaw size that can not grow to a critical flaw size within the time period to activate the radiation detector is justified. In this case, the radiation detector can activate the warning signal caused by coolant leakage from initially postulated flaws of the heat exchanger. The nuclear plant can safely shutdown when this occurs. Since the postulated initial flaw size can not grow to the critical flaw size, the structural integrity of the heat exchanger is not impeded. Particularly the informational scenario presented in this paper discusses an actual nuclear plant.

Key Words : Leak Before Break(LBB) Concept, Heat Exchanger, Finite Element Method (FEM), Plastic Stability, Structural Integrity Evaluation, Nuclear Power Plant

1. Introduction

A method to evaluate a structural integrity using the leak before break concept may not familiar to persons who are not involved in a nuclear power industry. The leak before break(LBB) concept is that an amount of leaking coolant from a pipe can be detected by a leak detection system before a pipe causes a catastrophical failure. The criterion to detect a leaking coolant is established as 37.9 ℓ/min with the plenty margin described in 10CFR GDC4(US Federal Register, 1986; 1987) published by United States Nuclear Regulatory Commission (USNRC).

* Corresponding Author,
E-mail : jdkwon@ynucc.yeungnam.ac.kr
TEL : +82-53-810-2462 ; **FAX** : +82-53-813-3703
School of Mechanical Engineering, Yeungnam University, 214-1, Dae-dong, Kyungsan, Kyungbuk 712-749, Korea. (Manuscript **Received** January 14, 2000; **Revised** October 16, 2000)

In order to explain and understand the LBB concept associated with a pipe, the critical flaw sizes, oriented to both axial and circumferential direction, must be obtained using existing fracture mechanics results. The leak rate calculation requires both the crack opening displacement(COD) and the crack opening area(COA). These two quantities are obtained using NUREG/CR-3464(Paris and Tada, 1983) associated with elastic analysis, elastic FEM and elastic-plastic FEM analysis. The PICEP computer code(Program, 1993) is used for leak rate calculation and this code is approved officially by USNRC. In order to perform the elastic-plastic FEM, a constitutive equation of the piping material is required. The Ramberg-Osgood equation of stainless steel TP304 is found using the curve fitting method from the stress-strain curve(Structural Alloys Hand Book, 1974). Using above mentioned procedures, crack lengths oriented both in the axial and the circumferential directions which can produce detectable leakage(37.9 ℓ/min) are found. The structural integ-

rity is justified by comparing the crack lengths which is able to detect the leak rate with the critical flaw sizes of given structure. The shape of crack opening area is assumed to be an elliptical shape and is able to find from the maximum crack opening displacement. These procedures explain very briefly for an application of the LBB to structural integrity evaluations.

The present paper is to apply LBB concept to a structure which is difficult to justify the structural integrity. Such structure is considered as a heat exchanger in nuclear power plants.

A heat exchanger in a nuclear power plant is a type of structure with a thin tube and a small diameter in order to improve heat exchange efficiency. The heat exchanger is difficult to apply the LBB concept as described in 10CFR GDC4 of the USNRC(US Federal Register, 1986; 1987) because the size of the heat exchanger is quite small and the leak rates are difficult to detect in a water environment. If a radiation warning instrument device is installed in or near the heat exchanger, then the alarm instrument will be triggered off by radiation energy that is in the coolant water that has leaked from the inside of the heat exchanger. Although this instrument exists already in operating plants and can serve as a device to detect coolant leakage, this paper explains one way to apply the LBB concept to structures which is not able to detect coolant leakage and small dimensional structures.

The primary coolant contains a radioactive material and the coolant flows into the inside of the heat exchanger. When the coolant leaks from the inside of the exchanger to the outside where there is low pressure and temperature, the radioactive material containing the primary coolant leaks. The radioactive material, on leaking to the outside of the exchanger and atmosphere, can be detected by the radiation detector installed near the exchanger. The minimum amount of coolant including the radioactive can be correlated with a certain amount of radiation. For example, the time required to reach 37.9 *liters* of coolant with radiation can be calculated. It all depends on the given size of the circumferential or longitudinal flaw. If the postulated size of the flaw can not increase to the critical flaw size obtained by Kanninen et. al.(1976) within the time period necessary to activate the radiation warning signal, then the nuclear plant shuts down as a result of the alarm signal. In this case, the structural integrity of the heat exchanger can be rationalized.

The value of 37.9 *liters* is conservatively estimated using the set point of a radiation warning system(RWS), 3×10^{-4} $\mu ci/cc$ which, for example, is the value of a nuclear plant and the radiation energy that emanates from the leaked coolant of the component cooling water heat exchanger(CCWHX). Since the radiation energy of the contaminated coolant is not known, the γ ray radiation energy of $^{60}_{27}Co$ is used in the calculation. Using this calculation, it is found that when a man, whose weight and surface area is 70 kg and 1.5 m^2, respectively, is exposed to this γ ray radiation energy for 1 year at a distance of 10 m from the source, the total energy received by the man is much less than the limit value of X-rays/year(70 *mrem/year* per person).

The paper describes a specific method to apply the LBB concept to a heat exchanger. The general purpose of the investigation is to show that a postulated circumferential or longitudinal flaw in the component cooling water(CCW) system heat exchanger tubes would leak out at a rate that would be detectable by the leak detection warning system that is an integral part of the heat exchanger. The leak detection device is actually a radiation detector installed in the vicinity of the exchanger. The present paper describes an alternative method to evaluate the integrity of structure which can not apply directly LBB concept. At author's best knowledge the method described in the paper is the first attempt to evaluate the integrity of structure with small dimensions in water environment in the country. However, whether this methods have been applied to such structure in the outside country, that is not known yet at author's knowledge. Particularly, the scenario presented in this paper is useful for an actual nuclear plant.

In order to achieve the present objective, the critical flaw size must be determined, along to the circumferential and the longitudinal directions,

using the actual dimensions of an excess letdown heat exchanger in a nuclear power plant. The method to calculate the critical flaw size is based on flaw stability using plastic hinge instability.

The crack opening displacement and crack opening area of the given flaw size of the pipe subjected to both internal and outside pressure are obtained using NUREG/CR-3464(Paris and Tada, 1983) and the FEM. The leak rates through cracks, oriented in both circumferential and longitudinal directions, are obtained using the PICEP leak rate calculation code(Program, 1993). Two kinds of leak rates are calculated. First, the leak rate is calculated using the crack opening displacement obtained by the inside program of the PICEP code. Secondly, the leak rate is found using the crack opening displacement obtained by the FEM and PICEP computer code. The structural integrity of the heat exchanger is evaluated applying the leak before break(LBB) concept.

The primary pressure from an excess letdown heat exchanger is 17.1 *MPa*. The secondary pressure from the excess letdown exchanger is 1 *MPa*. The unsupported span of the tube from a residual heat removal(RHR) heat exchanger is 622.3 *mm*. The tube size and thickness of the excess letdown heat exchanger are 15.9 *mm* and 1.7 *mm*, respectively. The design temperature from the excess letdown heat exchanger is 343.3℃. These data specifications are the dimensions of an actual, excess letdown heat exchanger in a nuclear power plant.

2. Critical Flaw Size Calculations

2.1 Critical flaw-size calculations in a circumferential orientation

The fracture which leads to failure in stainless steel must be determined using plastic methodology because of the large amount of deformation that occurs in a fracture. A conservative method for predicting the failure of ductile material is the plastic instability method. This method is based on the traditional plastic limit concepts. It accounts for strain hardening effect and takes into account the presence of flaws. A flawed tube is predicted for failure when the "remaining-net-section-reached" level at which a plastic hinge is formed. The stress level at which this occurs is termed "flow stress". The flow stress is generally taken as the average value of the yield and the ultimate tensile strength of the material at the selected temperature of interest. This methodology has been shown to be effective and applicable to ductile piping based on a large number of experiments(Kanninen et. al., 1976). It is used here to predict the critical flaw-size in the component cooling water(CCW), heat exchanger tube. The failure criterion has been obtained by requiring an equilibrium of the section which contains the flaw(Fig. 1) when various loads are applied. For throughwall circumferential cracks in a pipe with an internal pressure, axial force and imposed bending moments, the limit moment for these conditions is given as(Kanninen et. al., 1976),

$$M_b = 2\sigma_f r_m^2 t(2\cos\beta - \sin\alpha) \quad (1)$$

Table 1 Properties related to Eq. (1)

Notation	Unit	Value	Description
σ_f	*MPa*	$0.5(\sigma_y+\sigma_u)$	flow stress
σ_y	*MPa*	123.4(at 343.3 ℃) 172.4(at room temperature)	yield stress
σ_u	*MPa*	437.8	ultimate strength
r_m	*mm*	7.1	mean pipe radius
t	*mm*	1.7	pipe thickness
β	*rad*	$\alpha/2+(\pi r_i^2 P_i+F)/4\sigma_f r_m t$	angular location of neutral axis
α	*rad*	Half crack length/r_m	half angle of the crack(Fig. 1)
r_i	*mm*	6.25	inner pipe radius
P_i	*MPa*	17.1(design pressure) 21.4(testing pressure)	internal pressure
P_o	*MPa*	1	external pressure
F	*N*	0	axial force(except internal pressure)

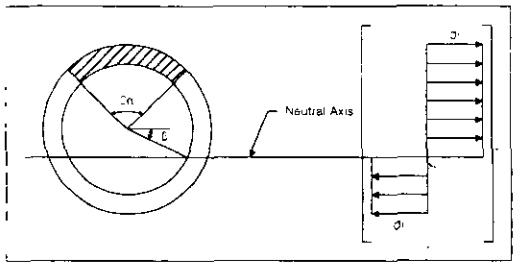

Fig. 1 Fully plastic stress distribution

Table 2 Properties related to Fig. 2

Notation	Unit	Value	Description
σ_f	*MPa*	280.6(at 343.3 ℃) 305.1(at room temperature)	flow stress $\sigma_f=0.5(\sigma_y+\sigma_u)$
Lc_1	*mm*	20.1(at 343.3 ℃)	critical flaw-size
Lc_2	*mm*	20.7(at room temperature)	(half of the crack length)

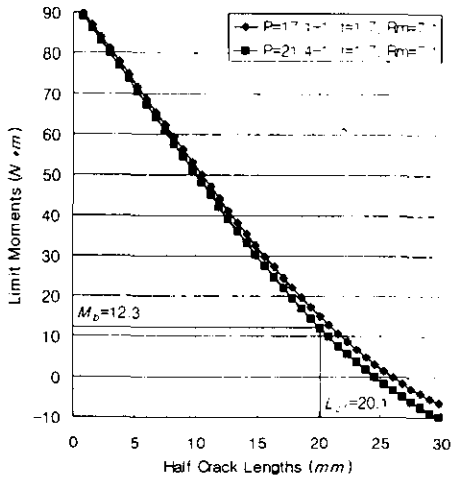

Fig. 2 Limit moments vs. half circumferential crack lengths ($\sigma_y=123.4$ *MPa*, $\sigma_u=437.8$ *MPa*)

The analytical model described by Eq. (1) accurately accounts for the piping internal pressure as well as imposed axial force as they affect the limit moment.

In order to validate the model, analytical predictions were compared with experimental results(Kanninen et. al., 1976). The results show good agreement with those obtained using Eq. (1). In order to calculate the critical flaw-size, a plot of the limit moment versus the crack length is required using Eq. (1), as shown in Fig. 2.

When the tube is subjected to only internal pressure, the tube is subjected to a zero moment. In this case, the external bending moment is considered as the bending moment, corresponding to the axial stress caused by the internal pressure. This is very conservative. The axial stress due to the internal pressure is given by,

$$\sigma=\frac{P_i r_m}{2t}\simeq\frac{21.4\times7.1}{2\times1.7}=46.1\ MPa \quad (2)$$

$$\sigma=\frac{MC}{I}\ \text{and}\ M_b=\frac{\sigma I}{r_m}=12.3\ N\cdot m \quad (3)$$

Table 3 Properties related to Eq.(4)

Notation	Unit	Value	Description
σ_L	*MPa*	$(1.28-1.4\lambda+0.809\lambda^2$ $-0.219\lambda^3+0.0217\lambda^4)\sigma_f$	limit axial stress($1\le\lambda\le5$)
λ		$a/\sqrt{r_m t}$	dimensionless number
a	*mm*		half crack length
r_m	*mm*	7.1	mean pipe radius
t	*MPa*	1.7	pipe thickness
σ_f	*MPa*	280.6(at 343.3 ℃) 305.1(at room temperature)	flow stress $\sigma_f=0.5(\sigma_y+\sigma_u)$

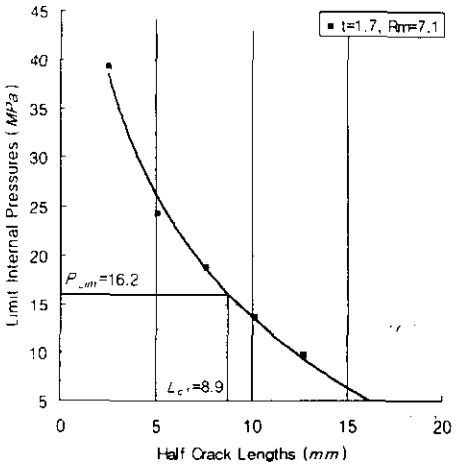

Fig. 3 Limit pressure variations with respect to axial crack lengths ($\sigma_y=123.4$ *MPa*, $\sigma_u=437.8$ *MPa*)

Using Eqs. (1) and (3), the intersection of the curve $M_b\sim r_m\alpha$ with $M_b=12.3\ N\cdot m$ is a half critical length, oriented in a circumferential direction. The flow stress and the critical flaw-size are shown in Table 2. The critical flaw-size, Lc_1 at 343.3 ℃ is found from Fig. 2 but Lc_2 at room temperature is not shown in Fig. 2.

2.2 Critical flaw-size calculations in a longitudinal orientation

The bending moment effects on a crack in the longitudinal orientation of a pipe is considered to be negligible. Thus, the internal pressure of the pipe is the predominant factor governing the limit load. The limit pressure variation, with repect to axial crack length, can be calculated from the following relationship(Bamford and Landerman,

1983):

$$P_{Lim}=\frac{\sigma_L t}{r_m} \tag{4}$$

where σ_L is expressed in Table 3.

The relationship between limit internal pressure, P_{Lim}(16.2 MPa) and a half of the crack length is shown in Fig. 3 at 343.3℃ and it can be obtained at room temperature using a similar method. Critical half crack lengths oriented in the longitudinal direction are found to be Lc_1=8.9 mm at 343.3℃ and Lc_2=9.6 mm, at room temperature (the result is not shown.).

3. Crack-Opening Area(COA) and Displacement(COD)

3.1 Crack-opening area oriented in a circumferential direction

The crack-opening area oriented in a circumferential direction is found using the expression given in Paris and Tada (1983). When the bending moment does not exist, the crack-opening area is given as,

$$A=\frac{\sigma}{E}(2\pi r_m t)G_p(\lambda),\ \lambda=a/\sqrt{r_m t} \tag{5}$$

where $\sigma=Pr_m/2t$, E=193.1 GPa (Young's modulus).

$$G_p(\lambda)=\lambda^2+0.16\lambda^4(0\le\lambda\le 1)$$
$$=0.02+0.81\lambda^2+0.303\lambda^3+0.03\lambda^4(1\le\lambda\le 5)$$

Equation (5) is obtained using elastic fracture mechanics. The crack-opening displacements are found, assuming the crack area is an elliptical shape.

3.2 Crack-opening area oriented in a longitudinal direction

Crack-opening area oriented in a longitudinal direction is found using the formula given in Paris and Tada (1983). When the bending moment is not present, the crack opening area is given as,

$$A=\frac{\sigma}{E}(2\pi r_m t)G(\lambda),\ \lambda=a/\sqrt{r_m t} \tag{6}$$

where $G(\lambda)=\lambda^2+0.625\lambda^4(0\le\lambda\le 1)$
$$=0.14+0.36\lambda^2+0.72\lambda^3$$
$$+0.405\lambda^4(1\le\lambda\le 5)$$

and $\sigma=Pr_m/t$

Equations (5) and (6) do not include plastic deformation at the crack tip. In order to compare the results obtained by Eqs. (5) and (6) with the FEM results, an FEM analysis is explained in the next section.

3.3 Finite element analysis

In order to find the accurate crack-opening area and displacement, oriented both in circumferential and longitudinal directions, the FEM is performed using the ABAQUS and includes strain hardening effects of the pipe(isotropic hardening). The stress-strain relationship of TP304 at room temperature is found in Structural Alloys Hand Book (1974). The stress-strain relationship is obtained by the curve fitting method. A comparison of the digitized stress-strain curve with that obtained by the curve fitting is shown in Fig. 4. The approximate stress-strain relationship is found to be,

$$\varepsilon/\varepsilon_y\cong\sigma/\sigma_y+7.1113\times10^{-4}(\sigma/\sigma_y)^{10} \tag{7}$$

In order to confirm the boundary conditions and the model of the FEM, the existing solutions(Paris and Tada, 1983) of the crack opening displacement(COD) are compared with that obtained by the FEM. The model employed in the FEM has a mean radius(r_m)=8 mm, t=

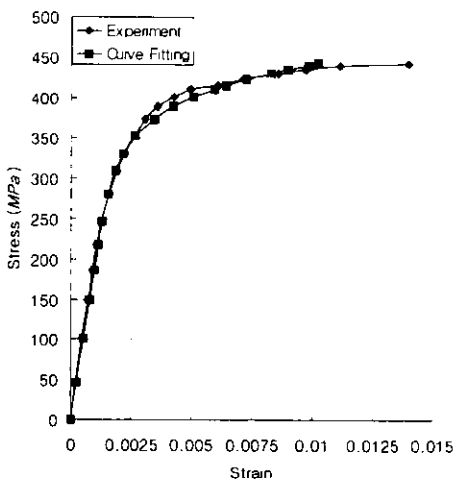

Fig. 4 Comparison of stress-strain curves obtained by experiments and curve fittings

Table 4 Properties related to Eq. (7)

Notation	Unit	Value	Description
ε_y		σ_y/E	elastic strain
σ_y	*MPa*	172.4(at room temperature)	yield stress
E	*GPa*	193.1	young's modulus

0.8 *mm*, and $L=254$ *mm*. This model shows that $r_m/t=10$ satisfies the definition of the thin shell. The COD obtained by Eq. (5) shows good agreement with that obtained by the FEM. It is common to use shell elements for the geometry of a cylinder with $r/t \geq 10$. Since the r_m/t of the present heat exchanger is 4.3 which is less than 10 in the finite element analysis, it is required to confirm whether or not shell elements can be employed in the FEM. The calculation of the FEM is performed using 2-D shell elements and 3-D solid elements. The CODs obtained by both 3-D solid and 2-D shell elements for the axial crack lengths 7.6 *mm* and 38.1 *mm*, respectively, are compared each other. The results show that the COD found in 2-D shell elements are approximately twice as large as those found in 3-D elements. Therefore, in this heat exchanger, 2-D shell elements may create errors in the numerical calculations and the FEM calculations are performed using 3-D solid elements. The node number and element number of quadratic, brick elements in the elastic analysis were of 16126 nodes and 3300 elements, respectively. If these mesh sizes are employed in the FEM for the plastic analysis, a tremendous amount of computation time is required since plastic analysis requires many iteration procedures.

Hence, the effort to reduce the number of nodes and elements is accomplished using a coarse mesh. The crack opening displacements of the pipe with an outside diameter of $D_0=19.1$ *mm*, the thickness of $t=3$ *mm* and the half pipe length $=95.3$ *mm* are calculated for the crack lengths of 7.6 *mm* and 38.1 *mm*, respectively. This takes place when using a coarse mesh which has 4811 nodes and 864 elements. The results obtained by a fine mesh which passed the convergence test are compared with those using the coarse mesh. The results fall into the 5~7.5% error range. Coarse

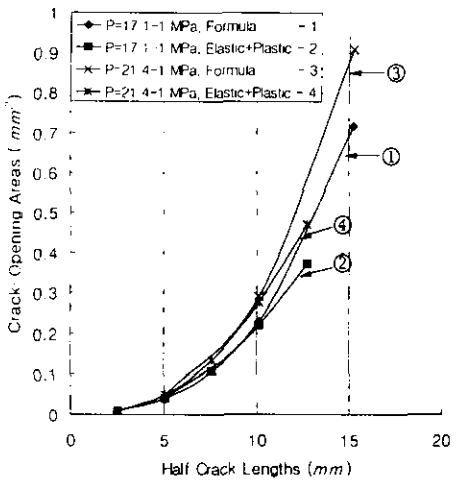

Fig. 5 Circumferential crack-opening areas ($r_m=7.1$ *mm*, $t=1.7$ *mm*)

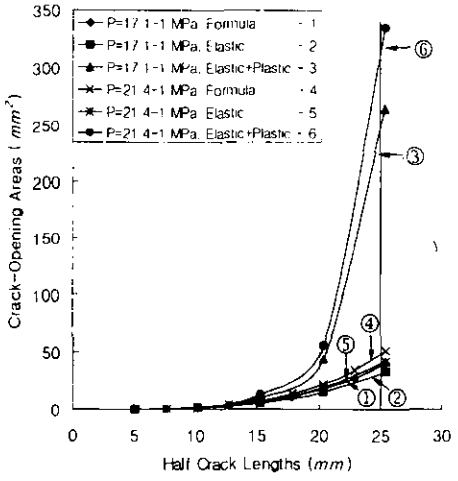

Fig. 6 Axial crack-opening areas ($r_m=7.1$ *mm*, $t=1.7$ *mm*)

mesh is employed in the present finite element analysis recognizing the fact that a degree of error may take place in the final results.

The crack opening areas obtained by the FEM are compared with those obtained using Eqs. (5) and (6). The results are shown in Figs. 5 and 6. However, the results of the FEM shows that the COD and the opening area of the circumferential crack obtained by the elastic FEM analysis are not at all different from those results obtained by the elastic-plastic FEM analysis. This result occurs when the range of the half crack length, is from 2.5 to 12.7 *mm*. It is noted that the compari-

son of the COD and the COA of the circumferential flaw obtained by the elastic and the elastic-plastic FEM analysis are not shown in Fig. 5.

The pronounced differences between the results of Eq. (5) and those of the elastic-plastic FEM analysis are recognized in large crack length, as noted in Fig. 5. It is found that the crack opening area obtained by Eq. (5) using the elastic the analysis is larger than the area obtained using the elastic-plastic FEM analysis, as shown in Fig. 5. The differences are caused by the value of r_m/t. Equation (5) is an approximate expression that is associated with a cylinder with $r_m/t=10$. When Eq. (5) is used for calculating the crack opening area of a cylinder with $r_m/t<10$, the crack opening area results into conservative values which are consistent with that described in NUREG/CR-3464(Paris and Tada, 1983). However, the axial crack opening area obtained by the elastic-plastic FEM analysis is much larger than that obtained by Eq. (6). Therefore, when Eq. (5) is used to calculate the crack opening area of the circumferential crack, caution is required for the value of r_m/t of an interested cylinder geometry.

The COD is found using FEM analysis. The leak rate of throughwall cracks that are oriented both in circumferential and axial direction for various crack lengths are found using the PICEP leak rate calculation code accepted by the USNRC.

4. Leak Rate Calculations

The purpose of this section is to discuss the method used to predict the flow through postulated cracks both in axial and hoop directions. The PICEP computer code is used for calculating the leak rate. This code is accepted for use by the USNRC. The detailed technical background and user's manual are described in the PICEP code(Program, 1993). The coolant is at a higher pressure state than the saturation pressure at the operating temperature and can be leaked through the throughwall cracks that are oriented in axial and hoop directions. When coolant is in a stagnated condition, it is in a liquid state and is called "a subcooled liquid". When the subcooled liquid starts to leak from throughwall cracks, the pressure rapidly drops in the thickness direction. This is caused by friction between the fluid motion and the roughness of crack surface. The fluid temperature can not be changed as the pressure drops because the fluid in the crack is surrounded by large amount of heat. Under these conditions, the pressure in the crack can arrive at the saturation pressure point corresponding to the fluid temperature. At this point, the subcooled liquid is changed to steam, which results into "a two phase flow". This phenomenon is termed as "flashing". The subcooled liquid remains in a liquid phase until flashing begins. The location at which flashing is initiated is approximately $L/D_h=40$,(L : crack length, D_h : hydraulic diameter). Pressure losses due to momentum changes will dominate when $L/D_h<40$ while friction pressure drop will become important when $L/D_h>40$. These conditions must be considered along with momentum losses that take place due to friction.

The PICEP code takes into account this physical phenomenon. The fracture mechanics, associated with the crack opening area or displacements, are able to calculate the leak rate at a particular given crack length.

The input data of the PICEP code has two options. The first option is to calculate the crack opening displacement using the inside of the PICEP code and takes into consideration the final crack length, the external loads and the Ramberg-Osgood equation, as shown in Eq. (7). The leak rate is calculated for various crack lengths. It is obtained by dividing the final crack length with a specific defined number taken from the input data. The other option is to calculate the leak rate. This can be found by using the input data of the COD and the crack length. The two options are used for the present calculations.

4.1 The results of the leak rate : Application of the LBB concept to heat exchanger structural integrity

The leak rate using the COD obtained by the FEM is calculated by the PICEP code with the COD of the FEM as input data. The leak rate using the COD obtained by the FEM is shown in

Fig. 7. This also includes the results of the COD obtained from the PICEP code. Figure 7 is the leak rate associated with an axial crack. If the crack length is less than 40.6 *mm*, the difference between the results of the FEM and the PICEP code is not significant. The difference is increased with the increasing lengths of cracks. For example, the leak rates obtained by using the COD of the PICEP code and the FEM at the axial full crack length, $2a$=45.7 *mm*, are approximately found in Fig. 7 as 89.9 ℓ/min and 184.8 ℓ/min, respectively. The ratio of the FEM result to that of PICEP code is 206%. When considering large crack lengths, it is found that the COD obtained by the FEM is larger in value than that calculated by the PICEP code. The leak rate from through-wall crack oriented in the circumferential direction is shown in Fig. 8. The difference between the leak rate obtained using the COD calculated by the FEM and that found from the PICEP code is increased with the length of the crack. The COD found from the FEM analysis is smaller than that obtained by the PICEP code in large size cracks (crack lengths $\geq$17.8 *mm*). The difference between the two results should be investigated further and with more depth.

The respective leak rates in the initial flaw sizes, 2.54, 5.08, 7.6 and 10.16 *mm* are found and those are shown in Figs. 7 and 8, and summarized in the Appendix, Table A. It is difficult to find the leak rates associated with small crack lengths as noted in Figs. 7 and 8. Therefore, the leak rates are directly found from the PICEP code output. The leak rate in the initial axial crack length, $2a$ =15.2 *mm*, for example, is found to be 1020.5 $m\ell/min$ using the COD obtained by the FEM. Using the COD obtained by the PICEP code, the leak rate is given as 1116.3 $m\ell/min$. The critical crack length given in Sec. 2.2 is $2a$=19.1 *mm* at room temperature and when at 343.3℃, $2a$=17.8 *mm*. Similarly, the leak rate of the circumferential initial crack length at $2a$=15.2 *mm*, as an example, is given as 57.5 $m\ell/min$ using the COD obtained by the FEM. Using the COD obtained by the PICEP code, the leak rate is given as 109.5 $m\ell/min$. The critical circumferential crack length given in Sec. 2.1 is 20.7 *mm* at room temperature and is 20.1 *mm* at 343.3℃.

If the leak rate of the circumferential flaw is smaller than that of the axial flaw, the failure caused by the fatigue crack growth in the circumferential direction is made greater than the growth in the axial direction since the longer time required to attain a critical flow of 37.9 *liters*

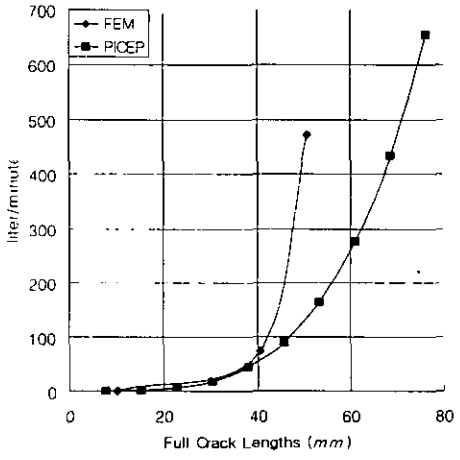

Fig. 7 Leak rate variations for various axial crack lengths (r_m=7.1 *mm*, t=1.7 *mm*)
FEM : COD is calculated by FEM, leak rates are obtained by PICEP
PICEP : COD is calculated by PICEP, leak rates are obtained by PICEP

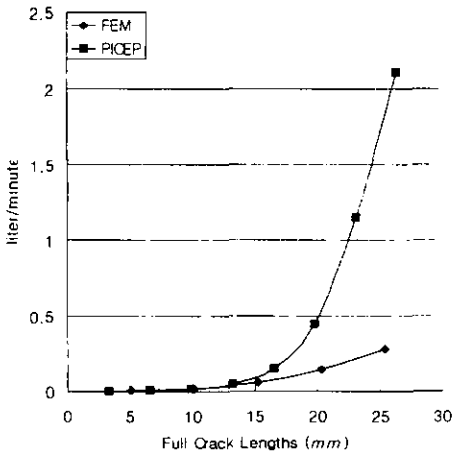

Fig. 8 Leak rate variations for various circumferential crack lengths (r_m=7.1 *mm*, t=1.7 *mm*)
FEM : COD is Calculated by FEM, leak rates are obtained by PICEP
PICEP : COD is calculated by PICEP, leak rates are obtained by PICEP

provides more opportunity for fatigue crack growth. Therefore, the smaller leak rate through the circumferential flaw is considered as the governing scenario for the present application of the LBB concept.

The fatigue loading causes the heat exchanger to be subjected to alternating stresses varying from the operating pressure to the ambient pressure. Therefore, it is required that the fatigue crack growth calculation considers the worst fatigue loading circumstance when the inside pressure of the heat exchanger fluctuates from atmospheric pressure to the original design pressure(17.1 *MPa*) and when the longitudinal stress amplitude is $\Delta S_a = P_i r_m / 2t = (17.1 \times 7.1)/(2 \times 1.7) = 34.7$ *MPa*. This $\Delta S_a = 34.7$ *MPa* is compared with ΔS_a in the S-N curve, as given in ASME Sec. III, Div. 1, Appendices. The results show that ΔS_a in S-N curve at 10^6 *cycles* is 194.4 *MPa* > 34.7 *MPa*, which means that the fatigue life of the heat exchanger, subjected to the worst transient scenario is infinite.

The fatigue crack growth caused by the worst transient of the heat exchanger is considered. The required time that the given crack size can grow to the critical crack size under the worst transient of the exchanger can be calculated using the fatigue crack growth law of stainless steel and is given as,(Bamford, 1979)

$$\frac{da}{dN} = 1.711 \times 10^{-17} (K_{eff})^{4.48} mm/cycl. \quad (8)$$

where $K_{eff} = MPa\sqrt{mm}$, a : crack size, N : number of cycle, $K_{eff} = K_{max}(1-R)^{1/2}$, and $R = K_{min}/$

Table A The time required to reach 37.9 *liters* and the time to reach FCG(Fatigue Crack Growth) relative to the circumferential critical crack length at various initial crack lengths

[1]Half crack lengths(*mm*)	PICEP		FEM				
	[2]COD (*mm*)	[2]*liters/minute*	COD (*mm*)	*liters/minute*	[3]Interpolated *liters/minute*	[4]37.9 *liters*/(*liters/minute*)(*hrs*)	[5]Time to a_{cr}(FCG)
1.27					0.00170	370	7.775×10^5 *hrs* (2.799×10^9 *cycles*)
2.54(a_1)	0.00173	0.00346	0.00191	0.00341		185	1.901×10^5 *hrs* (6.845×10^8 *cycles*)
3.81					0.00946	66	6.794×10^4 *hrs* (2.446×10^8 *cycles*)
5.08(a_2)	0.00483	0.01396	0.00484	0.01552		41	2.910×10^4 *hrs* (1.048×10^8 *cycles*)
6.35					0.03653	17	1.3401×10^4 *hrs* (4.824×10^7 *cycles*)
7.62(a_3)	0.00912	0.01095	0.00891	0.05754		11	6.80×10^3 *hrs* (2.19×10^7 *cycles*)
8.89					0.10107	6.2	2.317×10^3 *hrs* (8.341×10^6 *cycles*)
10.16(a_4)	0.03067	0.55214	0.01859	0.14460		4.4	2.36×10^2 *hrs* (8.485×10^5 *cycles*)

1), 2) : COD and *liters/minute* obtained by the various PICEP code are interpolated between the values of COD or *liters/minute* at crack lengths ;
$n\Delta a_i = n(33.02/10)$ *mm*.(n=1 to 10)

3) : *liters/minute* obtained by the PICEP code are linearly interpolated between *liters/minute* at the crack lengths a_{i+1} and a_i(a_0=0, i=0,1,2,3).

4) : Time required to reach 37.9 *liters*.

5) : Time required for FCG to occur from various initial crack lengths to the critical length a_{cr} under the assumption that the worst transient occurs every second.

K_{max}. The minimum inside pressure of the exchanger is atmospheric pressure and then axial stress, $\sigma=0$. So $K_{min}=0$, and $R=0$. The maximum stress intensity factor, K_{max} is equal to the stress intensity factor caused by the hoop stress that is created by the internal pressure. The maximum stress intensity factor is given in Paris and Tada (1983),

$$K_{1\max}=\sigma\sqrt{a}\,F_p(\lambda) \tag{9}$$

where $F_p(\lambda)=(1+0.3225\lambda^2)^{0.5}(0\leq\lambda\leq 1)$ and $F_p(\lambda)=0.9+0.25\lambda(\lambda=a/\sqrt{r_m t})(1\leq\lambda\leq 5)$

a is half crack length and the axial stress, $\sigma=P_i r_m/2t=34.7\ MPa$

Using Eqs. (8) and (9), the number of cycles required in which postulated various initial flaw sizes can grow to the critical size($a_{cr}/2=10.4$ *mm*) is estimated using the equation,

$$\int_{a_i}^{10.4}\frac{da}{a^{2.24}F_p(\lambda)^{4.48}}=(1.711\times10^{-17})(34.7)^{4.48}N \tag{10}$$

where a_i are the postulated initial flaw sizes and they are given in the Appendix, Table A.

If the worst transient is conservatively assumed to occur at every second, the various times required to grow from a_i to a_{cr} are estimated and those times are summarized in Table A. The time to grow from the postulated initial flaw, a_i to the next flaw, a_{i+1} as noted in Table A shows a much longer time period than that time needed to reach 37.9 *liters* through the initial flaw size, a_i. If the initial flaw size, $a=7.6$ *mm* which is arbitrarily selected and the conservative flaw size, oriented in the circumferential direction, is considered as an upper limit, then the RWS can be activated before all flaws, $a<7.6$ *mm* reach $a=7.6$ *mm*. Since $a=7.6\ mm<a_{cr}=10.4$ *mm*, the CCWHX can be shut down safely without impeding the structural integrity of the power plant. If a flaw $2a<15.2$ *mm* is detected, the plant can be operated continuously without repairing the exchanger until the flaw attains $2a=15.2$ *mm* with an appropriate safety margin$(a_{cr}=10.4)/(a=7.6)=1.37$. If $a=7.6$ *mm* is not selected and arbitrarily $a=5.08$ *mm* is considered then the safety margin increases to $10.4/5.08\approx 2$.

The value of 37.85 *liters*(37.9 *liters*) is estimated by the simple calculations noted below. The purpose of the calculations is to explain and justify a situation when a man whose weight is 70 *kg* with an approximate surface area of 1.5 m^2 is exposed to radiation energy at 10 *m* from the radiation source. This is dependent upon the man being safe based in the current dose limitation of radiation. Since the radiation energy contained in the coolant of the contaminated CCWHX is unknown, the γ ray energy radiated from the $^{60}_{27}Co$, 2.25 *Mev/dos*(Giancoli, 1995) is conservatively assumed. The limit to trigger the RWS is considered to be approximately 3×10^{-4} $\mu ci/cc$, an approximate example of a nuclear plant. When contaminated coolant(37.9 *liters* with 3×10^{-4} $\mu ci/cc$) is leaked, the coolant contains 11.36 *ci* which can be detected by the RWS. Half of the total γ ray energy is assumed to accumulate in the body. The energy contained in 37.85 *liters* of the CCW is found to be 1.05×10^6 *Mev/sec*. When the man is exposed to radiation at 10 *m* distance from the source, the total energy absorbed by the man is estimated to be $0.5\times(1.05\times10^6\ Mev/sec)\times(1.6\times10^{-13}\ J/Mev)\times(1.5\ m^2/(4\pi\times10^2\ m^2))=1.0\times10^{-10}\ J/sec$. Since 1 *gray*(*Gy*) is 1 *J/kg*, converting 1.0×10^{-10} *J/sec* to *Gy* unit is $1.0\times10^{-10}/70=1.44\times10^{-12}$ *Gy/sec*. The radiation energy exposure for 1 year is $1.44\times10^{-12}\times3600\times24\times365=4.54\times10^{-5}$ *Gy/yr*. Since 1 $Gy=100$ *rad* and $rem=rad\times QF$(quality factor=1), the exposed energy for 1 year can be converted to *rem* and it can be determined to be 4.54×10^{-3} $rad/yr=4.54$ *mrem*. This amount of radiation energy is much less than the energy exposed to *X*-rays per year corresponding to 70 *mrem/yr*. Therefore, 37.9 *liters*(10 *gallons*) to activate the RWS is fairly reasonable, conservatively-speaking.

When an arbitrarily selected initial flaw of $a=7.6$ *mm* is considered as an upper boundary to repair the flaw, twenty million cycles(Appendix, Table A) of the worst transient of the exchanger should take place within 11 *hrs* in order to impede the power plant's structural integrity. Based on the operating histories of the heat exchanger so far, it may be hardly expected that twenty million cycles of the worst transient takes

place within 11 *hrs*. Based on the stress corrosion mechanism, the operating history of PWR plants has shown no susceptibility to stress corrosion cracking for CCW heat exchanger tubes. Consequently, the leak before break principle can be applied to the CCW heat exchanger system.

5. Conclusions

The LBB concept is applied to a heat exchanger with thin tubes in a water environment. The critical crack sizes oriented in both the axial and circumferential directions are found using the existing expression(Kanninen et. al., 1976;Paris and Tada, 1983). The Ramberg-Osgood equation of TP304 stainless steel is obtained by digitizing the stress-strain relationship given in Structural Alloys Hand Book (1974). The crack opening area is found using Eqs. (5) and (6) that are expressed in Paris and Tada (1983). The crack opening displacement is found, assuming the shape of the opening area is an elliptical shape. The crack opening displacement and area are found using the FEM and the PICEP code. These results are compared in this paper. The application of the LBB concept to the CCW heat exchanger system is justified. Through analysis and calculations, the following conclusions are made :

(1) COD of axial cracks are affected by plastic deformation while circumferential cracks are not affected by plastic deformation. The opening area of a circumferential crack obtained by elastic FEM analysis is at the same magnitude as that obtained by elastic-plastic FEM analysis.

(2) The leak rate through the circumferential flaw obtained using the COD calculated by the FEM is smaller than that using the COD found from the PICEP code in the large cracks. The leak rate through an axial crack is larger than that in a circumferential crack using both COD found by the PICEP code and FEM.

(3) If the radiation detector installed in or near the heat exchanger is activated when the leaked coolant reaches a volume of 37.9 *liters*, the maximum time required for the 37.9 *liters* to go through the postulated initial circumferential crack length is much less than the time needed to grow to a critical flaw that has been caused by fatigue crack growth(see Table A in the Appendix). Consequently, the LBB principle can be applied to the CCW system heat exchanger tubes.

References

Bamford, W. H., 1979, "Fatigue Crack Growth of Stainless Steel Piping in a Pressurized Water Reactor Environment," *Trans. ASME J. of Pressure Vessel Technology*, Vol. 101., No. 5, p. 381.

Bamford, W. H. and Landerman, E. I., 1983, "Thermal Analysis of Cast Stainless Steel and Its Impact on Piping Integrity," *PVP*, Vol. 95, p. 143.

Giancoli, C. D., 1995, *Physics Principles with Application*, Prentice-Hall International, Inc. , New Jersey, pp. 1062~1065.

Kanninen, M. F., et al., 1976, "Mechanical Fracture Prediction for Sensitized Stainless Steel Piping with Circumferential Cracks," EPRI NP-192.

"Original-Pipe Crack Evaluation Program," 1993, Prepared by EPRI, Palo Alto, Calif., NP-3596-SR, Picep-Rev. 4.

Paris, P. C. and Tada, H., 1983, "The Application of Fracture Proof Design Methods Using Tearing Instability Theory to Nuclear Piping Postulating Circumferential Through Wall Cracks," NUREG/CR-3464.

"Structural Alloys Hand Book," 1974, Stainless 304, p. 61.

US Federal Register, 1986, Vol. 51, No. 70, 12502.

US Federal Register, 1987, Vol. 52, No. 207, 41288.